Holonomic Quantum Control with Continuous Variable Systems

Victor V. Albert,[1,*] Chi Shu,[1,2] Stefan Krastanov,[1] Chao Shen,[1] Ren-Bao Liu,[3] Zhen-Biao Yang,[1,4] Robert J. Schoelkopf,[1] Mazyar Mirrahimi,[1,5] Michel H. Devoret,[1] and Liang Jiang[1,†]

[1]*Departments of Applied Physics and Physics, Yale University, New Haven, Connecticut, USA*
[2]*Department of Physics, The Hong Kong University of Science and Technology, Hong Kong, China*
[3]*Department of Physics and Centre for Quantum Coherence, The Chinese University of Hong Kong, Hong Kong, China*
[4]*Department of Physics, Fuzhou University, Fuzhou, China*
[5]*INRIA Paris-Rocquencourt, Domaine de Voluceau, Le Chesnay Cedex, France*

(Received 10 April 2015; revised manuscript received 1 October 2015; published 7 April 2016)

Universal computation of a quantum system consisting of superpositions of well-separated coherent states of multiple harmonic oscillators can be achieved by three families of adiabatic holonomic gates. The first gate consists of moving a coherent state around a closed path in phase space, resulting in a relative Berry phase between that state and the other states. The second gate consists of "colliding" two coherent states of the same oscillator, resulting in coherent population transfer between them. The third gate is an effective controlled-phase gate on coherent states of two different oscillators. Such gates should be realizable via reservoir engineering of systems that support tunable nonlinearities, such as trapped ions and circuit QED.

DOI: 10.1103/PhysRevLett.116.140502

Reservoir engineering schemes continue to reveal promising new directions in the search for potentially robust and readily realizable quantum memory platforms. Such schemes are often described by Lindbladians [1] possessing decoherence-free subspaces (DFSs) [2] or (more generally) noiseless subsystems [3]—multidimensional spaces immune to the nonunitary effects of the Lindbladian and, potentially, to other error channels [4,5]. On the other hand, holonomic quantum computation (HQC) [6] is a promising framework for achieving noise-resistant quantum computation [7]. In HQC, states undergo adiabatic closed-loop parallel transport in parameter space, acquiring Berry phases or matrices (also called non-Abelian holonomies or Wilson loops [8]) that can be combined to achieve universal computation.

It is natural to consider combining the above two concepts. After the initial proposals [9,10], the idea of HQC on a DFS gained traction in Ref. [11,12] and numerous investigations into HQC on DFSs [13] and noiseless subsystems [14–16] followed. However, previous proposals perform HQC on DFS states constructed out of a finite-dimensional basis of atomic or spin states. There has been little investigation [17] of HQC on DFSs consisting of nontrivial oscillator states (e.g., coherent states [18,19]). While this is likely due to a historically higher degree of control of spin systems, recent experimental progress in the control of microwave cavities [20–22], trapped ions [23], and Rydberg atoms [24] suggests that oscillator-type systems are also within reach. In this Letter, we propose an oscillator HQC-on-DFS scheme using cat codes [Fig. 1(a)].

Cat codes are quantum memories for coherent-state quantum information processing [25], storing information in superpositions of well-separated coherent states that are evenly distributed around the origin of phase space. Cat-code quantum information can be protected from cavity dephasing via passive quantum error correction [26] using

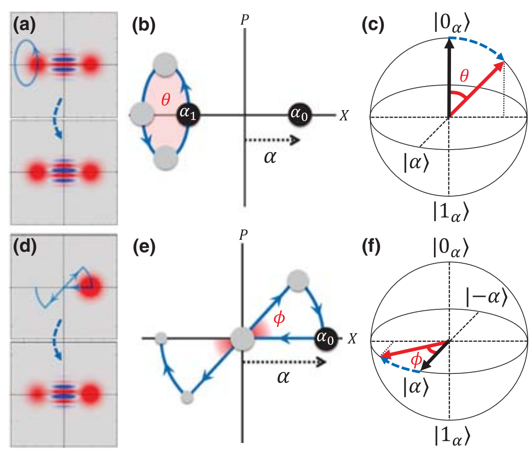

FIG. 1. In the $d = 2$ cat code, quantum information is encoded in the coherent states $|\alpha_0(0)\rangle \equiv |\alpha\rangle$ and $|\alpha_1(0)\rangle \equiv |-\alpha\rangle$. (a) Wigner function sketch of the state before (top) and after (bottom) a loop gate acting on $|-\alpha\rangle$, depicting the path of $|-\alpha\rangle$ during the gate (blue) and a shift in the fringes between $|\pm\alpha\rangle$. (b) Phase space diagram for the loop gate; $X = \frac{1}{2}\langle\hat{a} + \hat{a}^\dagger\rangle$ and $P = -(i/2)\langle\hat{a} - \hat{a}^\dagger\rangle$. The parameter $\alpha_1(t)$ is varied along a closed path (blue) of area A, after which the state $|-\alpha\rangle$ gains a phase $\theta = 2A$ relative to $|\alpha\rangle$. (c) Effective Bloch sphere of the $|\pm\alpha\rangle$ qubit depicting the rotation caused by the $d = 2$ loop gate. The black arrow depicts the initial state while the red arrow is the state after application of the gate. The dotted blue arrow does not represent the path traveled since the states leave the logical space $|\pm\alpha\rangle$ during the gate. (d)–(f) Analogous descriptions of the collision gate, which consists of reducing α to 0, driving back to $\alpha\exp(i\phi)$, and rotating back to α.

Lindbladian-based reservoir engineering [5]. In addition, such information can be actively protected from photon loss events [5,27–29]. While there exist plenty of methods to create and manipulate the necessary states [5,27,30–32] and while the gates can also be implemented using Hamiltonian control, we consider reservoir engineering due to its protective features. Cat codes differ from the well-known Gottesman-Kitaev-Preskill (GKP) encoding scheme [33] in both state structure and protection. GKP codes consist of superpositions of highly squeezed states and focus on protecting against small shifts in oscillator position and momentum. In contrast, cat codes protect against damping and dephasing errors, the dominant loss mechanisms for most cavity systems. While realistic GKP realization schemes remain scarce [34], cat codes benefit from greater near-term experimental feasibility [22].

For simplicity, let us introduce our framework using a single oscillator (or mode). Consider the Lindbladian

$$\dot{\rho} = F\rho F^{\dagger} - \frac{1}{2}\{F^{\dagger}F, \rho\} \quad \text{with} \quad F = \sqrt{\kappa}\prod_{\nu=0}^{d-1}(\hat{a} - \alpha_{\nu}), \tag{1}$$

$[\hat{a}, \hat{a}^{\dagger}] = 1$, $\hat{n} \equiv \hat{a}^{\dagger}\hat{a}$, $\kappa \in \mathbb{R}$, dimensionless $\alpha_{\nu} \in \mathbb{C}$, and ρ a density matrix. The $d = 1$ case $[F = \sqrt{\kappa}(\hat{a} - \alpha_0)]$ reduces to the well-known driven damped harmonic oscillator (see Ref. [35], Sec. 9.1) whose unique steady state is the coherent state $|\alpha_0\rangle$ (with $\hat{a}|\alpha_0\rangle = \alpha_0|\alpha_0\rangle$). Variants of the $d = 2$ case are manifest in driven two-photon absorption (see Ref. [36], Sec. 13.2.2), the degenerate parametric oscillator [see Ref. [37], Eq. (12.10)], and a laser-driven trapped ion [see Ref. [38], Fig. 2(d); see also Ref. [39]]. A motivation for this work has been the recent realization of the $F = \sqrt{\kappa}(\hat{a}^2 - \alpha_0^2)$ process in circuit QED [21], following an earlier proposal to realize $F = \sqrt{\kappa}(\hat{a}^d - \alpha_0^d)$ with $d = 2, 4$ [5]. For arbitrary d and certain α_{ν}, a qudit steady-state space is spanned by the d well-separated coherent states $|\alpha_{\nu}\rangle$ that are annihilated by F. The main conclusion of this work is that universal control of this qudit can be done via two simple gate families, *loop gates* and *collision gates*, that rely on adiabatic variation of the parameters $\alpha_{\nu}(t)$. Universal computation on multiple modes can then be achieved with the help of an entangling two-oscillator infinity gate. We first sketch the $d = 2$ case and extend to arbitrary d with $|\alpha_{\nu}\rangle$ arranged in a circle in phase space. The straightforward generalization to arbitrary arrangements of $|\alpha_{\nu}\rangle$ is presented in the Supplemental Material [40]. We then discuss gate errors and integration with cat-code error correction schemes [5,29], concluding with a discussion of experimental implementation.

Single-qubit gates.—Let $d = 2$ and let α_0, α_1 depend on time in Eq. (1), so the steady-state space holds a qubit worth of information. The positions of the qubit's two states $|\alpha_{\nu}(t)\rangle$ in phase space are each controlled by a tunable parameter. We let $\alpha_0(0) = -\alpha_1(0) \equiv \alpha$ (with α real unless stated otherwise). This system's steady states $|\pm\alpha\rangle$ are the starting point of parameter space evolution for this section and the qubit defined by them (for large enough α) is shown in Fig. 1(a).

The loop gate involves an adiabatic variation of $\alpha_1(t)$ through a closed path in phase space [see Fig. 1(b)]. The state $|\alpha_1(t)\rangle$ will follow the path and, as long as the path is well separated from $|\alpha_0(t)\rangle = |\alpha\rangle$, will pick up a phase $\theta = 2A$ with A being the area enclosed by the path [53]. It should be clear that initializing the qubit in $|-\alpha\rangle$ will produce only an irrelevant *overall* phase upon application of the gate (similar to the $d = 1$ case). However, once the qubit is initialized in a superposition of the two coherent states with coefficients $c_{\pm}$, the gate will impart a *relative* phase:

$$c_{+}|\alpha\rangle + c_{-}|-\alpha\rangle \to c_{+}|\alpha\rangle + c_{-}e^{i\theta}|-\alpha\rangle. \tag{2}$$

Hence, if we pick $|\alpha\rangle$ to be the x axis of the $|\pm\alpha\rangle$ qubit Bloch sphere, this gate can be thought of as a rotation around that axis [depicted blue in Fig. 1(c)]. Similarly, adiabatically traversing a closed and isolated path with the other state parameter $|\alpha_0(t)\rangle$ will induce a phase on $|\alpha\rangle$.

We now introduce the remaining Bloch sphere components of the cat-code qubit. For $\alpha = 0$, the $d = 2$ case retains its qubit steady-state space, which now consists of Fock states $|\mu\rangle$, $\mu = 0, 1$ (since $F = \sqrt{\kappa}\hat{a}^2$ annihilates both). One may have noticed that both states $|\pm\alpha\rangle$ go to $|0\rangle$ in the $\alpha \to 0$ limit and do not reproduce the $\alpha = 0$ steady-state basis. This issue is resolved by introducing the cat-state basis [54]

$$\begin{aligned} |\mu_{\alpha}\rangle &\equiv \frac{e^{-\frac{1}{2}\alpha^2}}{\mathcal{N}_{\mu}}\sum_{n=0}^{\infty}\frac{\alpha^{2n+\mu}}{\sqrt{(2n+\mu)!}}|2n+\mu\rangle \\ &\overset{\alpha\to\infty}{\sim} \frac{1}{\sqrt{2}}(|\alpha\rangle + (-)^{\mu}|-\alpha\rangle) \end{aligned} \tag{3}$$

with normalization $\mathcal{N}_{\mu} = \sqrt{\frac{1}{2}[1 + (-)^{\mu}\exp(-2\alpha^2)]}$. As $\alpha \to 0$, $|\mu_{\alpha}\rangle \sim |\mu\rangle$ while for $\alpha \to \infty$, the cat states (exponentially) quickly become "macroscopic" superpositions of $|\pm\alpha\rangle$. This problem thus has only two distinct parameter regimes: one in which coherent states come together ($\alpha \ll 1$) and one in which they are well separated ($\alpha \gg 1$, or more practically $\alpha \gtrsim 2$ for $d = 2$). Equation (3) shows that (for large enough α) cat states and coherent states become conjugate z and x bases, respectively, forming a qubit. We note that $\mu = 0, 1$ labels the respective ± 1 eigenspace of the parity operator $\exp(i\pi\hat{n})$; this photon parity is preserved during the collision gate.

We utilize the $\alpha \ll 1$ regime to perform rotations around the Bloch sphere z axis [Fig. 1(f)], which effectively induce a collision and population transfer between $|\alpha\rangle$ and $|-\alpha\rangle$. The procedure hinges on the following observation: applying a bosonic rotation $R_{\phi} \equiv \exp(i\phi\hat{n})$ to well-separated coherent or cat-state superpositions *does not* induce state-dependent phases, while applying R_ϕ to Fock state superpositions *does*. Only one tunable parameter $\alpha_0(t) = -\alpha_1(t)$ is necessary here, so $F = \sqrt{\kappa}[\hat{a}^2 - \alpha_0(t)^2]$ with $|\alpha_0(0)| = \alpha$. The collision gate consists of reducing α to 0, driving back to $\alpha \exp(i\phi)$, and rotating back to α [Fig. 1(e)]. The full gate is thus represented by $R_\phi^\dagger S_\phi S_0^\dagger$, with S_ϕ [55] denoting the nonunitary driving from 0 to $\alpha \exp(i\phi)$. Since

$$R_\phi^\dagger S_\phi S_0^\dagger = R_\phi^\dagger (R_\phi S_0 R_\phi^\dagger) S_0^\dagger = S_0 R_\phi^\dagger S_0^\dagger, \tag{4}$$

the collision gate is equivalent to reducing α, applying $R_\phi^\dagger$ on the steady-state basis $|\mu\rangle$, and driving back to α. The net result is thus a relative phase between the states $|\mu_\alpha\rangle$:

$$c_0|0_\alpha\rangle + c_1|1_\alpha\rangle \rightarrow c_0|0_\alpha\rangle + c_1 e^{-i\phi}|1_\alpha\rangle. \tag{5}$$

In the coherent state basis, this translates to a coherent population transfer between $|\pm\alpha\rangle$.

Two-qubit gates.—Now let us add a second mode $\hat{b}$ and introduce the entangling infinity gate for the two-photon case. We now use two jump operators for Eq. (1),

$$\begin{aligned} F_{\mathrm{I}} &= (\hat{a} - \alpha)(\hat{a} + \delta\alpha) \\ F_{\mathrm{II}} &= (\hat{a}\,\hat{b} - \alpha^2)(\hat{a}\,\hat{b} + \delta\alpha^2). \end{aligned} \tag{6}$$

We keep $\alpha > 0$ constant and vary $\delta(t)$ in a figure-eight or "∞" pattern (Fig. 2), starting and ending with $\delta = 1$. For $\delta = 1$, the four DFS basis elements $\{|\pm\alpha\rangle\} \otimes \{|\pm\alpha\rangle\}$ are annihilated by both F_{I} and F_{II}. For $\delta \neq 1$ and for sufficiently large α, the basis elements become $|\alpha,\alpha\rangle$, $|\alpha,-\delta\alpha\rangle$, $|-\delta\alpha,\alpha\rangle$, and $|-\delta\alpha,-\delta^{-1}\alpha\rangle$. Notice that the δ^{-1} makes sure that $F_{\mathrm{II}}|-\delta\alpha,-\delta^{-1}\alpha\rangle = 0$. This δ^{-1} allows the fourth state to gain a Berry phase distinct from the other three states. Since Berry phases of different modes add, we analyze the $\hat{a}/\hat{b}$-mode contributions individually. For any state that contains the $|-\delta\alpha\rangle$ component (in either mode), the Berry phase gained for each of the two circles is proportional to their areas. Since the oppositely oriented circles have the same area [Fig. 2(a)], these phases will cancel. The Berry phase of the fourth state, which contains the component $|-\delta^{-1}\alpha\rangle$, will be proportional to the total area enclosed by the path made by δ^{-1}. Inversion maps circles to circles, but the two inverted circles will now have *different* areas

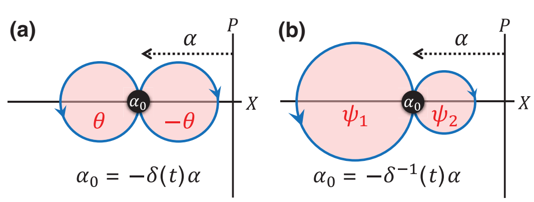

FIG. 2. Sketch of the adiabatic paths of the components (a) $|-\delta\alpha\rangle$ and (b) $|-\delta^{-1}\alpha\rangle$ during the infinity gate.

[Fig. 2(b)]. Summing the Berry phases ψ_i gained upon traversal of the two circles $i \in \{1,2\}$ yields an effective phase gate:

$$|-\alpha,-\alpha\rangle + |\mathrm{rest}\rangle \rightarrow e^{i(\psi_1+\psi_2)}|-\alpha,-\alpha\rangle + |\mathrm{rest}\rangle, \tag{7}$$

where $|\mathrm{rest}\rangle$ is the unaffected superposition of the remaining components $\{|\alpha,\alpha\rangle, |\alpha,-\alpha\rangle, |-\alpha,\alpha\rangle\}$.

Single-qudit gates.—We now outline the system and its single-mode gates for arbitrary d. Here, we let $\alpha_\nu(0) \equiv \alpha e_\nu$ with real non-negative α, $e_\nu \equiv \exp[i(2\pi/d)\nu]$, and $\nu = 0, 1, \ldots, d-1$ [see Fig. 3(a) for $d = 3$]. This choice of the initial qudit configuration makes Eq. (1) invariant under the discrete rotation $\exp[i(2\pi/d)\hat{n}]$ and is a bosonic analogue of a particle on a discrete ring [56]. Therefore, $\hat{n}\,\mathrm{mod}\,d$ is a good quantum number and we can distinguish eigenspaces of $\exp[i(2\pi/d)\hat{n}]$ by projections [57]

$$\Pi_\mu = \sum_{n=0}^{\infty} |dn+\mu\rangle\langle dn+\mu| = \frac{1}{d}\sum_{\nu=0}^{d-1} \exp\left[i\frac{2\pi}{d}(\hat{n}-\mu)\nu\right] \tag{8}$$

with $\mu = 0, 1, \ldots, d-1$. The corresponding cat-state basis generalizes Eq. (3) to

$$|\mu_\alpha\rangle \equiv \frac{\Pi_\mu|\alpha\rangle}{\sqrt{\langle\alpha|\Pi_\mu|\alpha\rangle}} \sim \begin{cases} |\mu\rangle & \alpha \to 0, \quad (9a) \\ \frac{1}{\sqrt{d}}\sum_{\nu=0}^{d-1} e^{-i\frac{2\pi}{d}\mu\nu}|\alpha e_\nu\rangle & \alpha \to \infty. \quad (9b) \end{cases} \tag{9}$$

Since the overlap between coherent states decays exponentially with α, the quantum Fourier transform between coherent states $|\alpha e_\nu\rangle$ and cat states $|\mu_\alpha\rangle$ in Eq. (9b) is valid in the well-separated regime, i.e., when $2\alpha\sin(\pi/d) \gg 1$ (satisfied when $|\langle\alpha|\alpha e_1\rangle|^2 \ll 1$). It should be clear that the more coherent states there are (larger d), the more one has to drive to resolve them (larger α). Also, note the proper convergence to Fock states $|\mu\rangle$ as $\alpha \to 0$ in Eq. (9a).

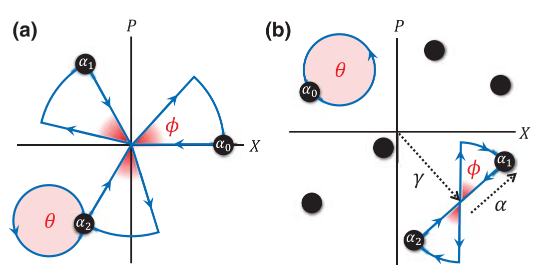

FIG. 3. (a) Threefold symmetric configuration of the steady states $|\alpha_\nu\rangle$ of Eq. (1) with $d = 3$ and depiction of a loop gate (θ) acting on $|\alpha_2\rangle$ and a collision gate (ϕ) between all states. (b) Arbitrary configuration of steady states for $d = 7$, depicting $|\alpha_0\rangle$ undergoing a loop gate and $|\alpha_1\rangle$, $|\alpha_2\rangle$ undergoing a displaced collision gate (see the Supplemental Material [40]).

Both gates generalize straightforwardly [see Fig. 3(a) for $d = 3$]. The loop gate consists of the adiabatic evolution of a specific $\alpha_\nu(t)$ around a closed path isolated from all other $\alpha_{\nu'}(0)$. There are d such possible evolutions, each imparting a phase on its respective $|\alpha e_\nu\rangle$. The collision gate is performed as follows: starting with the $|\alpha e_\nu\rangle$ configuration for large enough α, tune α to zero (or close to zero), pump back to a different phase $\alpha \exp(i\phi)$, and rotate back to the initial configuration. Each $|\mu_\alpha\rangle$ will gain a phase proportional to its mean photon number, which behaves in the two parameter regimes as follows:

$$\langle\mu_\alpha|\hat{n}|\mu_\alpha\rangle = \begin{cases} \mu + O(\alpha^{2d}) & \alpha \to 0, \quad (10a) \\ \alpha^2 + O(\alpha^2 e^{-c\alpha^2}) & \alpha \to \infty, \quad (10b) \end{cases} \tag{10}$$

where $c = 1 - \cos 2\pi/d$. Since a rotation imparts only a μ-independent (i.e., overall) phase in the well-separated regime [Eq. (10b)], the only μ-dependent (i.e., nontrivial) contribution of the symmetric collision gate path to the Berry matrix is at $\alpha = 0$. This gate therefore effectively applies the Berry matrix $\exp(-i\phi\hat{\chi})$ to the qudit, where $\hat{\chi} \equiv \sum_{\mu=0}^{d-1} \mu|\mu_\alpha\rangle\langle\mu_\alpha|$ is the discrete position operator of a particle on a discrete ring [56]. More generally, one does not have to tune α all the way to zero to achieve similar gates—e.g., being in the regime with $2\alpha\sin(\pi/d) \approx 1$ is sufficient. The two-mode infinity gate can likewise be extended to the d-photon case and it is a simple exercise to prove universality [40].

Gate errors.—In the Lindbladian-dominated adiabatic limit [40], the role of the excitation gap is played by the dissipation gap—the eigenvalue of the Lindblad operator whose real part is closest (but not equal) to zero. Since our Lindbladians are infinite dimensional, it is possible for the dissipation gap to approach zero for sufficiently large $|\alpha_\nu|$ (i.e., in the limit of an infinite-dimensional space). For the symmetric d-photon case however, this is not the case and the gap actually increases with α (verified numerically for $d \leq 10$). The gap can also be seen to increase by analyzing the excitation gap of the Hamiltonian $F^\dagger F$ (see Ref. [15], Sec. VIII.C). Having numerically verified the infinity gate, we also see that the gap increases with α in the two-mode system (6). Here, we discuss the scaling of leading-order nonadiabatic errors, focusing on the single-mode gates for $d = 2, 3$.

Nonadiabatic corrections in Lindbladians are in general nonunitary, so their effect is manifest in the impurity of the final state (assuming a pure initial state). Extensive numerical simulations [58] show that the impurity can be fit to

$$\epsilon \equiv 1 - \mathrm{Tr}\{\rho(T)^2\} \propto \frac{1}{\kappa T \alpha^p} \tag{11}$$

as $\alpha, T \to \infty$, where $\rho(T)$ is the state after completion of the gate, $\alpha \equiv |\alpha_\nu(0)|$ is the initial distance of all $|\alpha_\nu\rangle$ from the origin, $p > 0$ is gate dependent, and κ is the overall rate of Eq. (1). One can see that $\epsilon \approx O(T^{-1})$, as expected for a nearly adiabatic process. Additionally, we report that $p \approx 1.8$ for $d = 2$ and $p \approx 3.9$ for $d = 3$ loop gates, respectively. For the $d = 2$, 3 collision gates, we observe that $p \approx 0$.

Photon loss errors.—We have determined that the above gates can be made compatible with a (photon number) parity-based scheme protecting against photon loss [5,29]. In such a scheme, one encodes quantum information in a logical space spanned by even parity states (e.g., $|\alpha_\nu\rangle + |-\alpha_\nu\rangle$ with $\nu = 0, 1, \ldots, d-1$, generalizing Sec. II.D.3 of Ref. [26]). Photon loss events can be detected by quantum nondemolition measurements of the parity operator $(-1)^{\hat{n}}$. In the case of fixed-parity cat codes, errors due to photon loss events can be corrected immediately [29] or tracked in parallel with the computation [5]. By doubling the size d of the DFS of Lindbladian (1) to accommodate both even and odd parity logical spaces, we have determined a set of holonomic gates that are parity conserving and are universal on each parity subspace [40]. This scheme allows for parity detection to be performed before or after HQC.

Implementation and conclusion.—We show how to achieve universal computation of an arbitrary configuration of multimode well-separated coherent states $|\alpha_\nu\rangle$ by the adiabatic closed-loop variation of $\alpha_\nu(t)$. We construct Lindbladians that admit a decoherence-free subspace consisting of such states and whose jump operators consist of lowering operators of the modes. One can obtain the desired jump operators by nonlinearly coupling the multimode system to auxiliary modes $(\hat{c}, \hat{d}, \ldots)$, which act as effective thermal reservoirs for the active modes. For the case of one active mode $\hat{a}$, if one assumes a coupling of the form $\hat{a}\hat{c}^\dagger + \mathrm{H.c.}$ and no thermal fluctuations in $\hat{c}$, one will obtain (in the Born-Markov approximation) a Lindbladian with jump operator $\hat{a}$. Therefore, a generalization of the coupling to $F\hat{c}^\dagger + \mathrm{H.c.}$ will result in the desired single-mode Lindbladian (1) with jump operator F. Since the F are polynomials in the lowering operators of the active modes, quartic and higher mode interactions need to be engineered. Such terms can be obtained by driving an atom in a harmonic trap with multiple lasers [38] or by coupling between a Josephson junction and a microwave cavity [5,21]. We thus describe arguably the first approach to achieve holonomic quantum control of realistic continuous variable systems.

The authors thank S. M. Girvin, L. I. Glazman, N. Read, and Z. Leghtas for fruitful discussions. This work was supported by the ARO, AFOSR Multidisciplinary Research Program of the University Research Initiative, DARPA Quiness program, the Alfred P. Sloan Foundation, and the David and Lucile Packard Foundation. V. V. A. was supported by the NSF Graduate Research Fellowship Program under Grant No. DGE-1122492. C. S. was supported by the Paul and May Chu Overseas Summer Research Travel

Grant from HKUST and acknowledges support from Shengwang Du. R.-B. L. was supported by Hong Kong RGC/GRF Project No. 14303014. We thank the Yale High Performance Computing Center for use of their resources.

[*]valbert4@gmail.com
[†]liang.jiang@yale.edu

[1] V. Gorini, A. Kossakowski, and E. C. G. Sudarshan, J. Math. Phys. (N.Y.) **17**, 821 (1976); G. Lindblad, Commun. Math. Phys. **48**, 119 (1976).
[2] L.-M. Duan and G.-C. Guo, Phys. Rev. Lett. **79**, 1953 (1997); P. Zanardi and M. Rasetti, Phys. Rev. Lett. **79**, 3306 (1997); D. A. Lidar, I. L. Chuang, and K. B. Whaley, Phys. Rev. Lett. **81**, 2594 (1998).
[3] E. Knill, R. Laflamme, and L. Viola, Phys. Rev. Lett. **84**, 2525 (2000); P. Zanardi, Phys. Rev. A **63**, 012301 (2000); J. Kempe, D. Bacon, D. A. Lidar, and K. B. Whaley, Phys. Rev. A **63**, 042307 (2001).
[4] P. Zanardi and L. Campos Venuti, Phys. Rev. A **91**, 052324 (2015).
[5] M. Mirrahimi, Z. Leghtas, V. V. Albert, S. Touzard, R. J. Schoelkopf, L. Jiang, and M. H. Devoret, New J. Phys. **16**, 045014 (2014).
[6] P. Zanardi and M. Rasetti, Phys. Lett. A **264**, 94 (1999); J. Pachos, P. Zanardi, and M. Rasetti, Phys. Rev. A **61**, 010305 (1999); P. Zanardi, in *Quantum Error Correction*, edited by D. A. Lidar and T. A. Brun (Cambridge University Press, Cambridge, England, 2013), Chap. 16.
[7] P. Solinas, P. Zanardi, and N. Zanghì, Phys. Rev. A **70**, 042316 (2004).
[8] F. Wilczek and A. Zee, Phys. Rev. Lett. **52**, 2111 (1984).
[9] P. Zanardi, Phys. Rev. Lett. **87**, 077901 (2001).
[10] J. K. Pachos and A. Beige, Phys. Rev. A **69**, 033817 (2004).
[11] L.-A. Wu, P. Zanardi, and D. A. Lidar, Phys. Rev. Lett. **95**, 130501 (2005).
[12] A. Carollo, M. F. Santos, and V. Vedral, Phys. Rev. Lett. **96**, 020403 (2006).
[13] A. Carollo, G. Massimo Palma, A. Lozinski, M. F. Santos, and V. Vedral, Phys. Rev. Lett. **96**, 150403 (2006); X. D. Zhang, Q. Zhang, and Z. D. Wang, Phys. Rev. A **74**, 034302 (2006); Z.-Q. Yin, F.-L. Li, and P. Peng, Phys. Rev. A **76**, 062311 (2007); S. Dasgupta and D. A. Lidar, J. Phys. B **40**, S127 (2007); X.-L. Feng, C. Wu, H. Sun, and C. H. Oh, Phys. Rev. Lett. **103**, 200501 (2009); S.-B. Zheng, Phys. Rev. A **85**, 052106 (2012); **89**, 062118 (2014).
[14] O. Oreshkov, T. A. Brun, and D. A. Lidar, Phys. Rev. Lett. **102**, 070502 (2009); O. Oreshkov, Phys. Rev. Lett. **103**, 090502 (2009).
[15] O. Oreshkov and J. Calsamiglia, Phys. Rev. Lett. **105**, 050503 (2010).
[16] V. V. Albert, B. Bradlyn, M. Fraas, and L. Jiang, arXiv:1512.08079v2.
[17] D. Lucarelli and T. Tarn, in *Proceedings of the 41st IEEE Conference on Decision and Control* (IEEE, New York, 2002), Vol. 1, p. 452.
[18] A. Cacheffo, M. A. de Ponte, M. H. Y. Moussa, and A. S. M. de Castro, J. Phys. B **43**, 105503 (2010); G. D. M. Neto, A. Cacheffo, A. S. M. de Castro, M. A. de Ponte, and M. H. Y. Moussa, J. Phys. B **44**, 145502 (2011).
[19] M. A. de Ponte, S. S. Mizrahi, and M. H. Y. Moussa, Ann. Phys. (Amsterdam) **322**, 2077 (2007); J. Phys. B**41**, 215506 (2008); Phys. Rev. A **84**, 012331 (2011).
[20] C. Sayrin, I. Dotsenko, X. Zhou, B. Peaudecerf, T. Rybarczyk, S. Gleyzes, P. Rouchon, M. Mirrahimi, H. Amini, M. Brune, J.-M. Raimond, and S. Haroche, Nature (London) **477**, 73 (2011); G. Kirchmair, B. Vlastakis, Z. Leghtas, S. E. Nigg, H. Paik, E. Ginossar, M. Mirrahimi, L. Frunzio, S. M. Girvin, and R. J. Schoelkopf, Nature (London) **495**, 205 (2013); B. Vlastakis, G. Kirchmair, Z. Leghtas, S. E. Nigg, L. Frunzio, S. M. Girvin, M. Mirrahimi, M. H. Devoret, and R. J. Schoelkopf, Science **342**, 607 (2013); L. Sun, A. Petrenko, Z. Leghtas, B. Vlastakis, G. Kirchmair, K. M. Sliwa, A. Narla, M. Hatridge, S. Shankar, J. Blumoff, L. Frunzio, M. Mirrahimi, M. H. Devoret, and R. J. Schoelkopf, Nature (London) **511**, 444 (2014); R. W. Heeres, B. Vlastakis, E. Holland, S. Krastanov, V. V. Albert, L. Frunzio, L. Jiang, and R. J. Schoelkopf, Phys. Rev. Lett. **115**, 137002 (2015).
[21] Z. Leghtas, S. Touzard, I. M. Pop, A. Kou, B. Vlastakis, A. Petrenko, K. M. Sliwa, A. Narla, S. Shankar, M. J. Hatridge, M. Reagor, L. Frunzio, R. J. Schoelkopf, M. Mirrahimi, and M. H. Devoret, Science **347**, 853 (2015).
[22] N. Ofek, A. Petrenko, R. Heeres, P. Reinhold, Z. Leghtas, B. Vlastakis, Y. Liu, L. Frunzio, S. M. Girvin, L. Jiang, M. Mirrahimi, M. H. Devoret, and R. J. Schoelkopf, arXiv:1602.04768.
[23] J. T. Barreiro, M. Müller, P. Schindler, D. Nigg, T. Monz, M. Chwalla, M. Hennrich, C. F. Roos, P. Zoller, and R. Blatt, Nature (London) **470**, 486 (2011); P. Schindler, M. Müller, D. Nigg, J. T. Barreiro, E. A. Martinez, M. Hennrich, T. Monz, S. Diehl, P. Zoller, and R. Blatt, Nat. Phys. **9**, 361 (2013).
[24] A. Signoles, A. Facon, D. Grosso, I. Dotsenko, S. Haroche, J.-M. Raimond, M. Brune, and S. Gleyzes, Nat. Phys. **10**, 715 (2014).
[25] S. Haroche and J.-M. Raimond, *Exploring the Quantum: Atoms, Cavities, and Photons* (Oxford University Press, Oxford, 2006); H. Jeong and T. C. Ralph, in *Quantum Information with Continuous Variables of Atoms and Light*, edited by N. J. Cerf, G. Leuchs, and E. S. Polzik (World Scientific, London, 2007), Chap. 9.
[26] B. M. Terhal, Rev. Mod. Phys. **87**, 307 (2015).
[27] P. T. Cochrane, G. J. Milburn, and W. J. Munro, Phys. Rev. A **59**, 2631 (1999).
[28] S. Glancy, H. M. Vasconcelos, and T. C. Ralph, Phys. Rev. A **70**, 022317 (2004).
[29] Z. Leghtas, G. Kirchmair, B. Vlastakis, R. J. Schoelkopf, M. H. Devoret, and M. Mirrahimi, Phys. Rev. Lett. **111**, 120501 (2013).
[30] H. Jeong and M. S. Kim, Phys. Rev. A **65**, 042305 (2002); T. C. Ralph, A. Gilchrist, G. J. Milburn, W. J. Munro, and S. Glancy, Phys. Rev. A **68**, 042319 (2003); A. Gilchrist, K. Nemoto, W. J. Munro, T. C. Ralph, S. Glancy, S. L. Braunstein, and G. J. Milburn, J. Opt. B: Quantum Semiclass. Opt. **6**, S828 (2004); A. Ourjoumtsev, R. Tualle-Brouri, J. Laurat, and P. Grangier, Science **312**, 83 (2006); M. Takeoka and M. Sasaki, Phys. Rev. A **75**,

064302 (2007); A. P. Lund, T. C. Ralph, and H. L. Haselgrove, Phys. Rev. Lett. **100**, 030503 (2008); H. Takahashi, K. Wakui, S. Suzuki, M. Takeoka, K. Hayasaka, A. Furusawa, and M. Sasaki, Phys. Rev. Lett. **101**, 233605 (2008).

[31] W. J. Munro, G. J. Milburn, and B. C. Sanders, Phys. Rev. A **62**, 052108 (2000).

[32] C. Arenz, C. Cormick, D. Vitali, and G. Morigi, J. Phys. B **46**, 224001 (2013); M. J. Everitt, T. P. Spiller, G. J. Milburn, R. D. Wilson, and A. M. Zagoskin, Front. ICT **1**, 1 (2014).

[33] D. Gottesman, A. Kitaev, and J. Preskill, Phys. Rev. A **64**, 012310 (2001).

[34] B. M. Terhal and D. Weigand, Phys. Rev. A **93**, 012315 (2016).

[35] A. B. Klimov and S. M. Chumakov, *A Group-Theoretical Approach to Quantum Optics* (Wiley, Weinheim, 2009).

[36] R. R. Puri, *Mathematical Methods of Quantum Optics* (Springer, Berlin, 2001).

[37] H. J. Carmichael, *Statistical Methods in Quantum Optics 2: Non-Classical Fields* (Springer-Verlag, Berlin, 2008).

[38] J. F. Poyatos, J. I. Cirac, and P. Zoller, Phys. Rev. Lett. **77**, 4728 (1996).

[39] B. M. Garraway, P. L. Knight, and M. B. Plenio, Phys. Scr. **T76**, 152 (1998); A. R. R. Carvalho, P. Milman, R. L. de Matos Filho, and L. Davidovich, Phys. Rev. Lett. **86**, 4988 (2001).

[40] See Supplemental Material at http://link.aps.org/supplemental/10.1103/PhysRevLett.116.140502, which cites Refs. [41–52], for an extension of the infinity gate to qudits, a proof of universal computation, a generalization to arbitrary $|\alpha_\nu\rangle$, a sketch of the derivation of the Berry matrices, and details on how to integrate the gates with a photon loss error correction scheme.

[41] E. B. Davies and H. Spohn, J. Stat. Phys. **19**, 511 (1978); P. Thunstrom, J. Aberg, and E. Sjoqvist, Phys. Rev. A **72**, 022328 (2005); J. P. Pekola, V. Brosco, M. Möttönen, P. Solinas, and A. Shnirman, Phys. Rev. Lett. **105**, 030401 (2010).

[42] S. Lloyd, Phys. Rev. Lett. **75**, 346 (1995).

[43] J. E. Avron, M. Fraas, and G. M. Graf, J. Stat. Phys. **148**, 800 (2012).

[44] M. S. Sarandy and D. A. Lidar, Phys. Rev. A **71**, 012331 (2005).

[45] M. S. Sarandy and D. A. Lidar, Phys. Rev. A **73**, 062101 (2006).

[46] J. E. Avron, M. Fraas, G. M. Graf, and O. Kenneth, New J. Phys. **13**, 053042 (2011); J. E. Avron, M. Fraas, G. M. Graf, and P. Grech, Commun. Math. Phys. **314**, 163 (2012).

[47] L. Campos Venuti, T. Albash, D. A. Lidar, and P. Zanardi, Phys. Rev. A **93**, 032118 (2016).

[48] G. F. Xu, J. Zhang, D. M. Tong, E. Sjöqvist, and L. C. Kwek, Phys. Rev. Lett. **109**, 170501 (2012); S. L. Wu, L. C. Wang, and X. X. Yi, J. Phys. A **45**, 405305 (2012); G. Xu and G. Long, Sci. Rep. **4**, 6814 (2014); Z.-T. Liang, Y.-X. Du, W. Huang, Z.-Y. Xue, and H. Yan, Phys. Rev. A **89**, 062312 (2014); V. A. Mousolou, C. M. Canali, and E. Sjöqvist, New J. Phys. **16**, 013029 (2014); P. V. Pyshkin, D.-w. Luo, J. Jing, J. Q. You, and L.-A. Wu, arXiv:1507.00815; Z.-Y. Xue, J. Zhou, and Y. Hu, arXiv:1601.07219.

[49] J. Zhang, L.-C. Kwek, E. Sjöqvist, D. M. Tong, and P. Zanardi, Phys. Rev. A **89**, 042302 (2014).

[50] S. L. Braunstein and P. V. Loock, Rev. Mod. Phys. **77**, 513 (2005).

[51] A. Beige, D. Braun, B. Tregenna, and P. L. Knight, Phys. Rev. Lett. **85**, 1762 (2000); D. Burgarth, P. Facchi, V. Giovannetti, H. Nakazato, S. Pascazio, and K. Yuasa, Phys. Rev. A **88**, 042107 (2013).

[52] P. Facchi and S. Pascazio, Phys. Rev. Lett. **89**, 080401 (2002); G. A. Paz-Silva, A. T. Rezakhani, J. M. Dominy, and D. A. Lidar, Phys. Rev. Lett. **108**, 080501 (2012).

[53] S. Chaturvedi, M. S. Sriram, and V. Srinivasan, J. Phys. A **20**, L1071 (1987).

[54] V. V. Dodonov, I. Malkin, and V. Man'ko, Physica (Utrecht) **72**, 597 (1974).

[55] When acting on states in the DFS, S_ϕ can be approximated by a path-ordered product of DFS projections $P_\alpha = |0_\alpha\rangle\langle 0_\alpha| + |1_\alpha\rangle\langle 1_\alpha|$ with each projection incrementing α: $S_\phi \approx P_{\alpha e^{i\phi}} \cdots P_{(2/M)\alpha e^{i\phi}} P_{(1/M)\alpha e^{i\phi}}$ for integer $M \gg 1$ [4]. Using Eq. (3), one can show that $P_{\alpha e^{i\phi}} = R_\phi P_\alpha R_\phi^\dagger$ and prove Eq. (4).

[56] A. Vourdas, Rep. Prog. Phys. **67**, 267 (2004).

[57] V. V. Albert and L. Jiang, Phys. Rev. A **89**, 022118 (2014).

[58] S. Krastanov, "Animations of cat-qudit gates", http://dancingblobs.krastanov.org/.